

Supplementary Material: Formation of amorphous multi-walled carbon nanotubes from random initial configurations

*Chinonso Ugwumadu**, *Rajendra Thapa*, *David A. Drabold*

C. Ugwumadu, Prof. D. A. Drabold
Department of Physics and Astronomy,
Nanoscale and Quantum Phenomena Institute (NQPI),
Ohio University, Athens, Ohio 45701, USA
E-mail: cu884120@ohio.edu

Dr. R. Thapa
Institute for Functional Materials and Devices
Lehigh University, Bethlehem, PA 18015, USA

Keywords: *amorphous solids, nanotubes, carbon*

Sect. S1 Description of Animations produced for the amorphous Nanotubes (a-CNT) models

We have produced some animations to aid the reader in visualizing some of the discussions in the paper. The animations can be found [here](#) or by visiting the url: <https://people.ohio.edu/drabold/nanotubes/>

The descriptions are as follows:

1. **README.txt**: File containing similar descriptions of the animations written here.
2. **Hollow_a-CNT_mov.mp4**: This describes the formation process of hollow a-CNT.
3. **Capped_a-CNT_mov.mp4**: This describes the formation process of capped a-CNT.
4. **PiBandDensity_mov.mp4**: This shows the variations in the π electron distribution along the z-direction of an a-CNT₄₀₀ model, the slices are perpendicular to the z-direction as shown in the image (a-CNT_400atoms.jpg) attached to the animation.
5. **freq_vibrations.mp4**: This shows the evolution of all vibrational modes in a-CNT, from high frequency (in-plane) to low frequency (out-of-plane) to Goldstone modes (collective vibrations).
6. **freq_11.mp4**: One of the Goldstone modes. This helps to compare other low-frequency modes to a typical Goldstone mode
7. **freq_32.mp4**: Twisting vibrational frequency of the outer tube, the inner tube does not move
8. **freq_44.mp4**: Translational vibration of inner tube
9. **freq_55.mp4**: Twisting vibrational frequency of the inner tube, the outer tube does not move
10. **freq_81.mp4**: Collective low-frequency radial breathing mode (RBM) of both tubes in the a-DWCNT
11. **freq_807.mp4**: Resonant mode (quasi-localized modes that diffuse away) since the VIPR ≈ 0.15 at this frequency.
12. **freq_1746.mp4**: Localized high frequency optic-like mode. The vibrating atoms are in red and the direction of vibration is specified using arrows

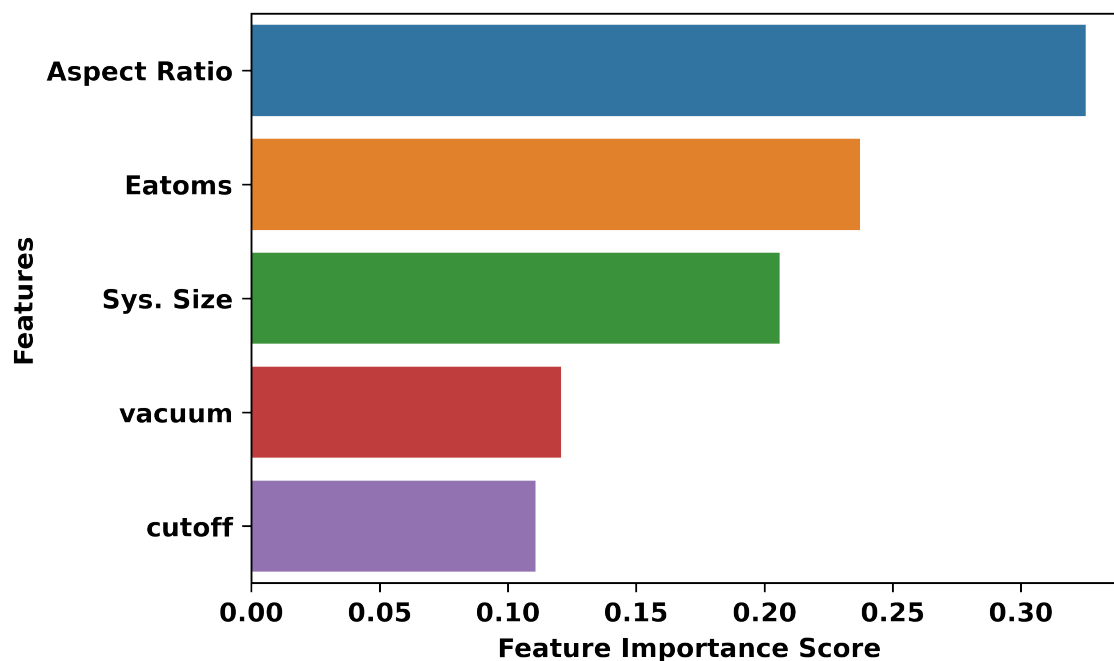


Figure S1: Average feature importance score from 20 instances of the RF classifier using the Gini impurity index.

Sect. S2 Random Forest Implementation for Important variables in a-CNT Formation

For the random forest (RF) implementation, a number of features were modified to reduce correlation in the data. For example, the height and diameter of the starting configuration were replaced by an aspect-ratio, which in turn can define the number density. Fig. S1 shows the averaged importance profile of the features and the Gini score for a 4-fold cross-validation set is shown as a radar chart in Fig. S2. Fig. S3 shows the binary decision tree for a-CNT formation on a training set using only aspect-ratio and system size with an accuracy score of 0.93. We stress that our interest lies majorly in the important-feature predictive power of RF. This aided in narrowing the window of tunable variables required to investigate significant physical characteristics in our simulations. 634 models were used for training and the system sizes were selected randomly from a range of 200 - 3200 atoms. The aspect ratio was sampled from a normal distribution ($\mu = 4.3$, $\sigma = 1.2$) to sample only positive values.

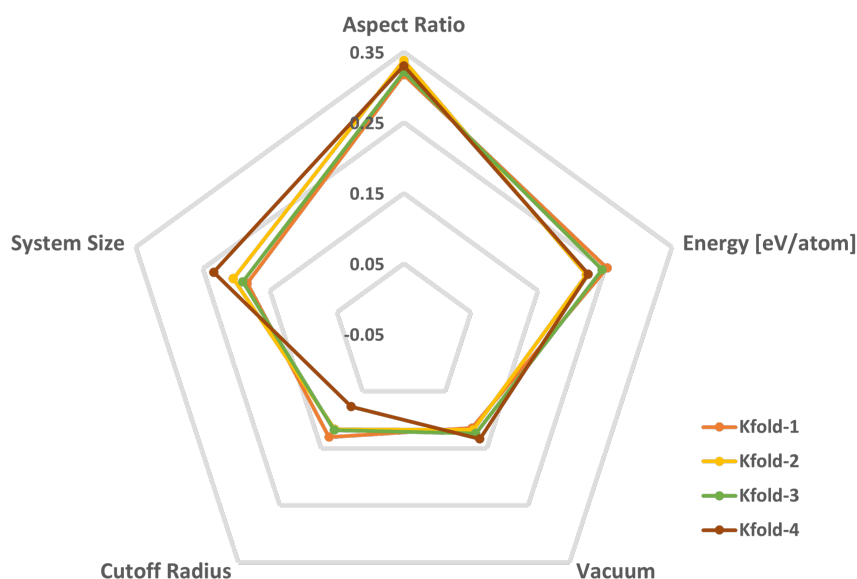


Figure S2: Radar Chart showing the important features from K-fold cross-validation ($K = 4$) of a random forest classifier using the Gini index.

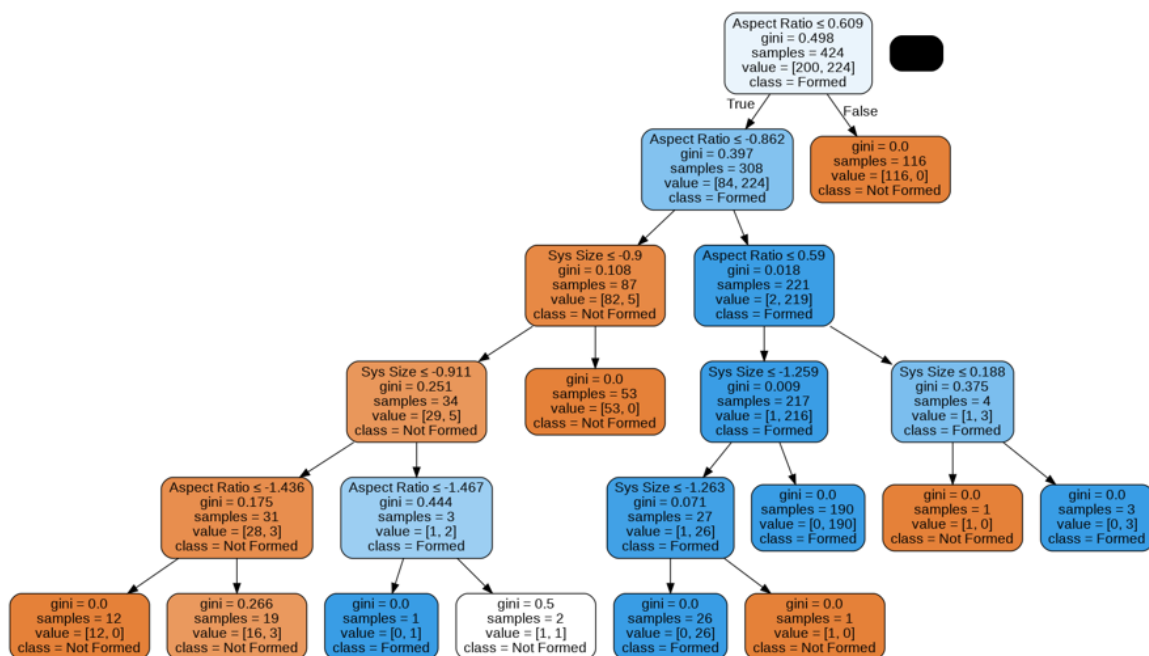


Figure S3: visualization of the decision tree for a binary classifier using the aspect ratio and system size. "Formed" class indicates that a-CNT is formed and the "Not Formed" class indicates otherwise. see Fig. S4 for examples of such models.

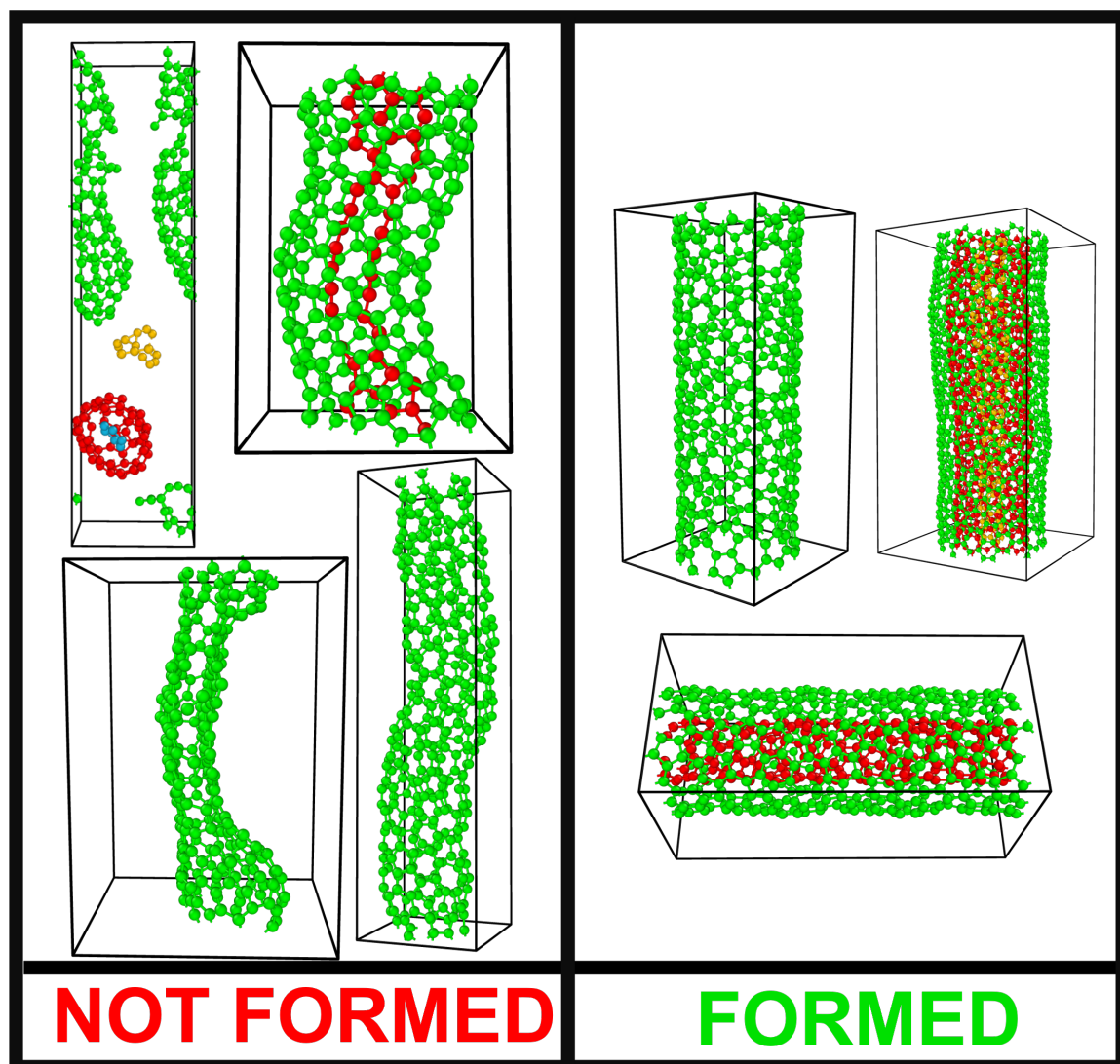


Figure S4: Examples of models that do not form [LEFT] and models that form [RIGHT] a-CNT based on their input variables

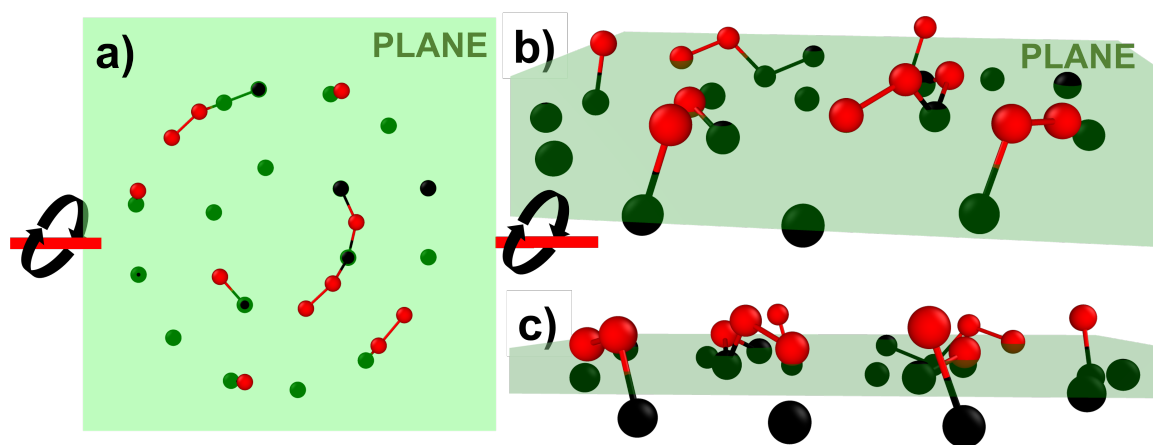


Figure S5: Visualization of the atoms contributing to the π electron cloud in the slice discussed in the manuscript. In (a) the black (gray) atoms are below (above) the slice plane. The CW rotation of (a), along the horizontal axis of the plane (shown in red solid lines), is shown in (b) (45° CW) and (c) (90° CW). Atoms that fall right on the plane (see c) are also colored in black.

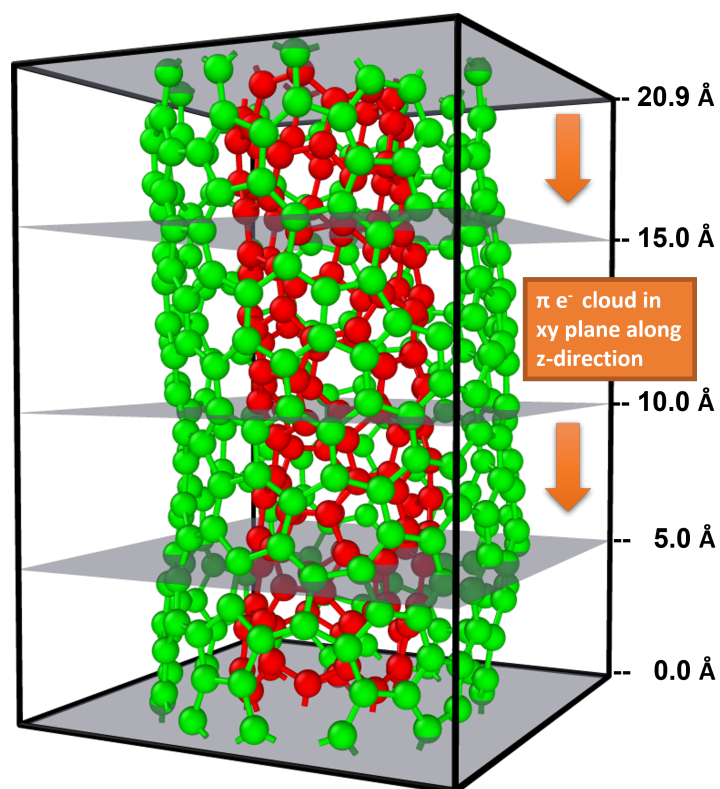


Figure S6: Figure showing the direction of slicing for one of the a-CNT₄₀₀ models used in the analysis of the π electron density distribution.